

Stage de recherche de deuxième année du MIP

MARS - AOUT 2004

Thibaut DIVOUX

Listening to singing bubbles at the free surface of a non-newtonian fluid

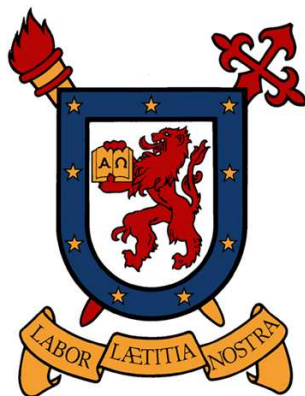
En écoutant chanter les bulles

Sous la direction de :

Francisco MELO

&

Jean-Christophe GEMINARD



Universidad de Santiago de Chile

Laboratorio de Física No Lineal,
Center for Advanced Interdisciplinary Research in Materials (CIMAT),
Avenida Ecuador 3493,
Casilla 307 Correo 2,
SANTIAGO-CHILE

Abstract

Sound produced by gas emission through a fluid layer, in the context of volcanic eruption is not yet fully understood. Strombolian explosions consist in the breaking of large overpressurized bubbles at the surface of the magma column, which produces two monochromatic signals. In order to enlight the relationship between seismic spectral contents and the physical nature of bursting bubbles, we decide to focus on the sound emitted by a single bursting bubble at the free surface of a hair-Gel solution. The use of a non-newtonian fluid takes into account foam properties of lava.

Rising in a Gel solution, an overpressurized bubble develops a sharp centimetre tail. Reaching the fluid free surface, a thin film separates the bubble from the bulk air. The breaking of the thin film excites the cavity limited by the bubble walls. As elastic properties of our Gel solutions allow the bubble tail being motionless during this excitation, the bubble tail plays the role of a resonating tube, emitting a sound (audible high frequency). Afterwards, a damped shear elastic wave takes place while the bubble inner-walls fall down (low frequency). A single bursting bubble at the free surface of a non-newtonian fluid produce two signals of well defined frequency, and thus could be at the origin of the two well-defined frequencies recorded on the top of the volcanoes vent.

We also present a simple device dealing with soap film breaking under tubes of variable lengths. These tubes are perfect bubbles of controled properties which confirm us the energy is stocked with the overpressure, and mainly released by radiations. This system allows us to develop some intuitions about the more complicated bubble system.

Résumé

Lors des éruptions volcaniques, du gaz est amené à traverser les couches de lave pour être libéré bruyamment en surface. Une partie de l'activité du Stromboli consiste en l'explosion de larges bulles surpressurisées à la surface de colonnes de laves, qui produisent deux signaux de caractère monochromatique. Ayant dans l'idée de préciser la relation existant entre la nature des explosions (bulles) et le spectre des signaux associés, nous nous sommes penchés sur les signaux émis lors de l'explosion d'une bulle d'air surpressurisée à la surface d'un fluide non-newtonien : du Gel pour les cheveux. L'utilisation de Gel nous permet de prendre en compte les propriétés viscoélastiques de la lave.

Une bulle d'air qui monte dans une colonne de Gel developpe une queue pointue de l'ordre du centimètre. En atteignant la surface, un film fin de Gel séparant la bulle de l'air extérieur se forme, puis se rompt excitant la queue conique de la bulle. Les propriétés élastiques du Gel permettent à cette queue de ne pas se déformer durant toute la vidange de la bulle. Elle joue alors le rôle d'un résonateur émettant un son (haute fréquence audible). Puis les parois de la bulle s'effondrent en s'affaissant, générant une onde élastique de cisaillement (basse fréquence). Ainsi, l'explosion d'une bulle d'air à la surface d'un fluide non-newtonien produit deux signaux de fréquences bien définies qui pourraient être à l'origine des signaux enregistrés à la surface des conduits de lave.

Nous exposons parallèlement un petit montage permettant d'écouter la rupture de films de savons sur des tubes de plexiglass de longueurs variables. Ces tubes et films peuvent être vus comme des "bulles parfaites" au sens où nous en contrôlons les propriétés géométriques. Un bilan d'énergie nous permet alors de développer quelque intuition sur l'explosion des bulles qui reste plus complexe.

Acknowledgements

Ces remerciements se feront en français pour être au plus juste de ma pensée.

Ce travail de maîtrise, essentiellement expérimental a été effectué au sein du groupe non-linéaire de l'USACH à Santiago. Comme un enfant, j'ai eu la chance de grandir durant 6 mois auprès de Francisco et Jean-Christophe. Au milieu de gouttes de sables grimpanes et de coquilles d'oeufs cassés, Jean-Christophe m'a proposé d'écouter chanter des bulles. Merci à toi de m'avoir fait confiance en me proposant ce sujet qui te tenait à coeur depuis quelques temps. Merci pour tout ce temps passé à discuter de bulles et de bien plus. Tu sais à quel point ces discussions ont nourri mes réflexions. Francisco m'a accueilli avec enthousiasme et simplicité. Merci d'avoir trouvé le temps d'être présent et actif dans un emploi du temps presque inhumain. Les quelques idées théoriques soulevées et développées dans ce travail sont le fruit de réflexions communes réelement enrichissantes. Tous deux expérimentateurs brillants, vous avez su nourrir ma passion de l'expérience que vous saviez éclore. Merci pour votre profonde et desarçonnante humilité.

Un grand merci à toute la petite équipe du Labo. Erika pour son efficacité et la joie dispensée sans compter, Pancho pour sa compétence et ses nombreux dépanages PC. Merci à Stephane pour son franc-parlé quotidien, Eugenio pour ses remarques ponctuelles. Merci à Leo pour ses conseils culinaires, et à Roberto pour les petits croissants. Enfin merci à Jorge pour ses soins très paternels.

Ces 6 mois n'auraient certainement pas eu la même résonance sans ma petite famille Chilienne. Gracias a Erwin y Margarita por recibirme como su tercero hijo. Gracias a Erwin hijo por iluminar mi vida diaria, Ingrid por introducirme en la musica Chilena y Hermann-sito por su humor. Fue muy grata vivir con vosotros. Merci à Ludovic pour les nocturnes citadines et les nombreux week-ends itinérants. De San Pedro à Chiloé, tu sais comme tes coups de gueules et nos silences partagés ont été essentiels à mes changements.

Un petit clin d'oeil à Kenneth et Martin pour les articles envoyés quelle que soit l'heure du jour...ou de la nuit.

Ma présence au Chili a été en partie financée par le *Fondo de Investigación Avanzada en Areas Prioritarias Grant 11980002 (2004)*

Introduction

Fluid flows are described by the continuous set of Navier Stokes equations. This description remains fruitful as long as microscopic and macroscopic scales remain separated. Thus, problems appear on the one hand as soon as flow sizes are reduced to the flow particle one; typically when a drop detaches from a capillary under gravity, singular behaviors known as finite-time singularity ensue [1]. On the other hand, increasing fluid-particles size affords greater degrees of freedom which leads to macroscopic viscoelasticity [5]. Complex fluids as polymers and wormlike micelles solutions satisfy this size effects. Under flow, polymers react by bending their statistical equilibrium pelota-shape on time scale allowing matter-flow interaction. The added feature of self-assembling micelles is that their length distribution is determined by aggregation kinetics, thus micelles continually break and reform [7, 8, 28]. In both cases, increasing particle size, introduces one (polymers) or two (micelles) time scales to the relevant physical parameters. Those new time scales allow spectacular macroscopical effects as the Weissenberg effect. A rotating cylinder in an elastic fluid will not dig a hole in the free surface, but make the fluid climb along the cylinder [5]. "Die swell effect" is of the same kind (fig. 1).

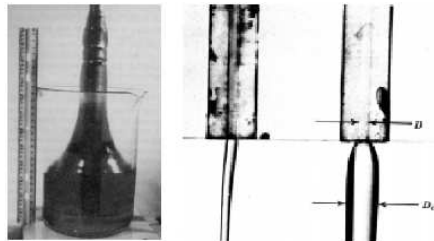


FIG. 1 – *The Weissenberg effect (Left); "die swell effect" (Right) occurs with fluid presenting strong and anisotrope elastic stress coming out of a capillary tube [5].*

Several novel results have been reported : dealing with falling hanging drop, the finite-time singularity occuring with water drop has been drastically inhibited using polymer solutions [2] or presheared micelles solutions [11]. Notice here that two properties going the same way (produce a finite-time singularity), lead to an inhibition of this effect. Also, falling spheres [16] and rising air-bubbles [15] in micelles solutions have been observed to oscillate without reaching a terminal velocity. And while rising, an air-bubble displays a sharp and non-axisymmetric cusp, which remains unchanged during a steady rise [5]. Bubbles in non-newtonian fluids have been studied for the past ten years : modeling and understanding bubbles formation [20]; correlating bubbles rise [21] and coalescence [22] with local change of fluid structures involving stress competing mechanism. Finally, a liquid film separates air bubbles from the bulk air at the surface of viscous liquids. These long-lifetime films display unusual dynamical behaviors in drainage and rupture [9, 10]. Air-bubbles collect and explode this way at the surface of lava flow during volcanic eruptions.

For instance, Strombolian activity consists in a series of explosions due to the breaking of large overpressurized bubble at the surface of the magma column which produces two monochromatic acoustic signals. The signal of lower frequency could be explained by vibration [30, 32] or coalescence [26] of bubbles under the free surface. A large agreement seems to link the upper frequency to bubbles explosions themselves [26, 31, 32] : this frequency is independant of the geometrical features of the volcanic conduit, and the pressure in the lava column seems to control the explosivity of the Stromboli [24, 27]. However the relationship between seismic spectral content and physical nature of the source remains unclear and unknown : why recorded signals present two well defined frequencies ? And as lava is a foam,

Can a single bubble bursting at the free surface of a non-newtonian fluid produce two sounds of well defined frequencies ? Or vibrations, and coalescence hypothesis remain necessary.

To answer these questions we are going to listen to bubbles bursting at the free surface of a non-

newtonian fluid. From now on, two points of view can be adopted : a phenomenological one consists in listening to a permanent regime of bursting bubbles. Air is permanently injected in the system and bubbles are allowed to interact : rising bubbles may form new structure : connected long chains similar to beads [18]. These air tunnels have a proper sound emission, and require to listen globally to hours of signals, and thousands of events [33]. Having the choice, a physicist would prefer the second approach which consists in listening and understanding the explosion of a single bubble at the surface of a non-presheared and non-newtonian fluid.

Contents of this report

Part ONE focuses on the high frequency a bursting bubble produces. We show that the bubble while exploding, behaves as an undeformable resonator excited by the tearing of the thin film separating the bubble from the bulk air. We introduce rough estimates and simple ideas on bursting bubbles.

In **Part TWO**, we dwell on the thin film properties and on the way its breaking stimulates the resonator. A simple soap film breaking device is presented to establish general results on film - resonator interaction, and achieve simple energy balances.

Part THREE allows us to enlight the bubble bursting sound with soap film result. The competition between characteristic times allows the energy emitted by bursting bubbles to present an optimum varying bubbles volume for a given Gel concentration.

Finally, **Part FOUR** sums up the low frequency properties : a shear elastic wave takes place after the bubble has collapsed.

The way the report is written should not appear weird. This 6 month work has been mainly spent in hours of experiments, looking for the simplest way to prove (or infirm) ours intuitions and the most scientific way to shot a bursting bubble. I do hope this report to give the reader the feeling he's reading a story book of simple, but not so dead easy experiments. Being more formal would have drawn this "short novel". Going trough it, I hope you will take as much pleasure and astonishment as I did, living and writing it.

I) Learning about the high frequency

Experiments are conducted in a plexiglas rectangular column ($30 \times 30 \times 88 \text{ mm}$). The cell is fulfilled with a hair-Gel solution (*Gel fijador para el cabello, for men, Camel White*®), and air-bubbles are generated by means of a submerged orifice at the bottom section of the column using calibrated syringes, with total volumes ranging from 3 to 50 mL. We watch and listen to bubbles exploding at the free surface on the top of the cell. Pictures and films are recorded using a fast camera Hisis 2002 that makes possible to capture 100 to 1220 frames per second. Sound is recorded with an electrostatic microphone (used with appropriate conditioning and amplification units); associated signals are visualized with an oscilloscope and archived using a simple code under *labview*. If necessary sounds and frames are synchronised using a homemade comparator circuit : the sound emission triggers a LED visible on frames, marking a zero (fig. 10).

Hair-Gel solutions ranging from 25 to 45 % Gel concentration, are prepared with distilled water and mixed during half a day using a stirring rod. Submitting the solutions to ultrasonic sound, remaining bubbles are destroyed . Finally, the solutions are left at rest a night before performing experiments. As the solutions dry up significantly after a week and a half, we do not work more then four days with the same solution.

For this first part, we listen to a single bubble rising through a non presheared hair-gel solution. Actually, as our solutions are shear thinning¹, a bubble rising through a non presheared hair-Gel solution creates a privileged path for other bubbles that will rise after it, at least before the solution relaxes. Bubbles of the same volume rising through a presheared and a non presheared solution do not rise the same way. In sheared areas, viscosity decreases leading to bubbles of higher velocity, and very different shape (fig. 2). In order to perform experiments in the same conditions for all bubbles, we could have wait a few relaxation times of our hair-Gel solution. However, this time lasts more than a few minutes and we prefer stirring slowly the solution, destroying that way the presheared path ².

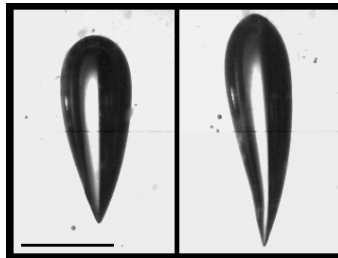


FIG. 2 – A 0.70 mL rising bubble in a 40 % Gel solution. Left : the Gel is not presheared, the bubble is creating a sheared conduct. Right : bubble evolving in this conduct ; the bubble is getting thinner and will explode at the free surface with other geometrical properties than the left-hand bubble (scale : black straight line is worth 1 cm).

After formation, a bubble rises through the gel oscillating as mentioned by Belmonte, and the cusp periodically extends to a sharp point and then retracts to a blunt edge [15]. The bubble then reaches the free surface which deforms : while at rest, a thin film separates the bubble from the bulk air. Actually, we observe two distinct behaviours : a bubble rising in a low Gel-concentration solution ($\leq 30\%$) stands a few seconds to a few minutes in equilibrium at the surface before exploding (*regime 1*), whereas bubbles rising through a high Gel concentration solution ($\geq 30\%$) explode immediately when reaching the free surface (*regime 2*).

¹The viscosity of the solution decreases while increasing the shear-ratio.

²This way, we certainly do preashear a bit the whole Gel solution. But after a few stirring, the solution reaches some stationary states, and repeating an experiment leads to the same results. We thus kept this method.

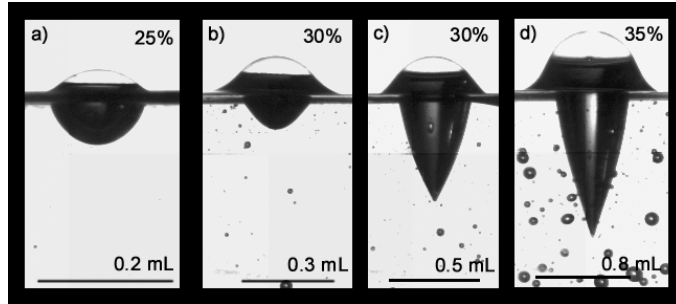


FIG. 3 – Bubbles shapes for 3 concentrations and 4 representative volumes. The a) and d) pictures illustrate namely regime 1 & 2 varying Gel concentration and volume. Centered pictures c) and d) illustrate a regime change at fixed concentration. In the last right-hand-side picture, we can see small bubbles emphasizing the threshold property. (scale : black straight lines are worth 1 cm.)

Nevertheless the gel concentration of the solutions is not the only relevant parameter as for intermediate concentration of 30% Gel, the solution exhibits both behaviours, depending on the volume of air injected : meaning that "small bubbles" have a rest at the surface before their film breaks, while "big bubbles" do not (fig. 3). This volume-driven transition is hardly brought to the fore for concentrations higher than 30 % because of the threshold properties of our solutions. A way to enlight this transition is to look at the parameter drastically changing with the volume : the total vertical length of the bubble, before explosion L_b (fig. 4).

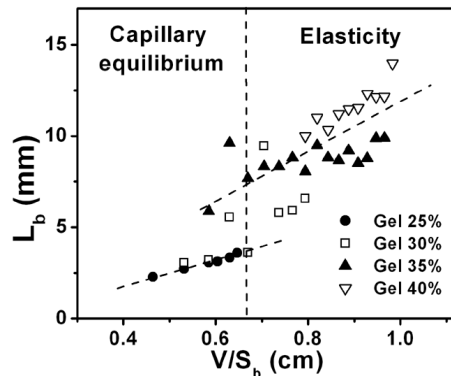


FIG. 4 – The length L_b before explosion (± 0.4 ms) versus the bubble volume V . As the bubble section before explosion S_b varies slightly with V , we divide V by S_b . The shape-transition introduced on figure 3 is clearly visible as the graph parts in two regions. Left-hand-side region ruled by capillarity allows the bubble to rest, while right-hand-side region do not, and is ruled by elasticity.

Figure 4 exhibits two different regimes :

- the left part of the graph corresponds to low Gel concentration solutions with water like properties. Bubbles have small volumes³ and low overpressure. Bubbles reach an equilibrium at the free surface, and their shape is almost driven by surface tension. The radius of curvature allows us to evaluate surface tension. For instance, the picture a) of figure 3 gives a fair $\gamma \simeq 20$ mN/m, a weak-but-correct value for water surface-tension with surfactants.
- the right part of the graph corresponds to high Gel concentration solutions, with high elastic properties. Evaluating the surface tension of the solution for a bubble at the border of the two regimes gives an absurd $\gamma \simeq 80$ mN/m $\gg 20$ mN/m (second left picture of figure 3) as the surface tension of Gel solutions of concentrations ranging from 25 to 40 % is almost the same. This evaluation only involves gravity and surface tension which hence shows that elastic stress rules capillarity for Gel

³capillarity makes bubbles of higher volumes break into smaller ones during their rise.

concentrations higher than 30 %. Overpressure required to create bubbles in such solutions makes them unable to rest on the fluid surface before breaking.

At the free surface, capilarity balances the Archimediuss forces. And as both regimes present a flow in the thin film which separates the bubble from the bulk air, an effective surface tension balances the Archimediuss forces ($\gamma_{eff} \gg \gamma_{water}$). Consequently, a bubble smaller than the effective capillar length $\kappa^{-1} = \sqrt{\gamma_{eff}/\rho g}$ will have a rest at the free surface, whether larger bubbles will not⁴.

Finally, we can associate a tail shape before film breaking to both regimes. Bubbles having a rest at the surface present a round bottom, whether the others present a sharp one. This fact can be intuitively understood⁵. At low Gel concentration⁶, the local pressure equilibrium of a bubble, which gravity center is at the depth h can be written as :

$$\rho g h = 2\gamma \left(\frac{1}{R_u} - \frac{1}{2R_l} \right) \quad (1)$$

writing bubble inner-pressure two different ways, with R_u and R_l namely the upper and lower radius of curvature. As the left-hand is positive, $2R_l$ has to be greater than R_u , unless what no closed physical shape should exist for the bubble tail as the pressure is not locally equilibrated. This is the case for every rising bubbles whatever its overpressure is : the dynamics sets the sharp shape of the bubble tail, which presents a singularity at its very end.

In both regimes, a bursting bubble is accompanied by the emission of a high and well defined frequency. Ranging from 1 to 10 kHz, the frequency range is obtained varying two parameters : the bubbles volume and the Gel concentration of our solutions. In figure 5, we report the typical bubbles shapes and signals emitted for solutions of 25, 30, 35 and 40 % Gel concentrations.

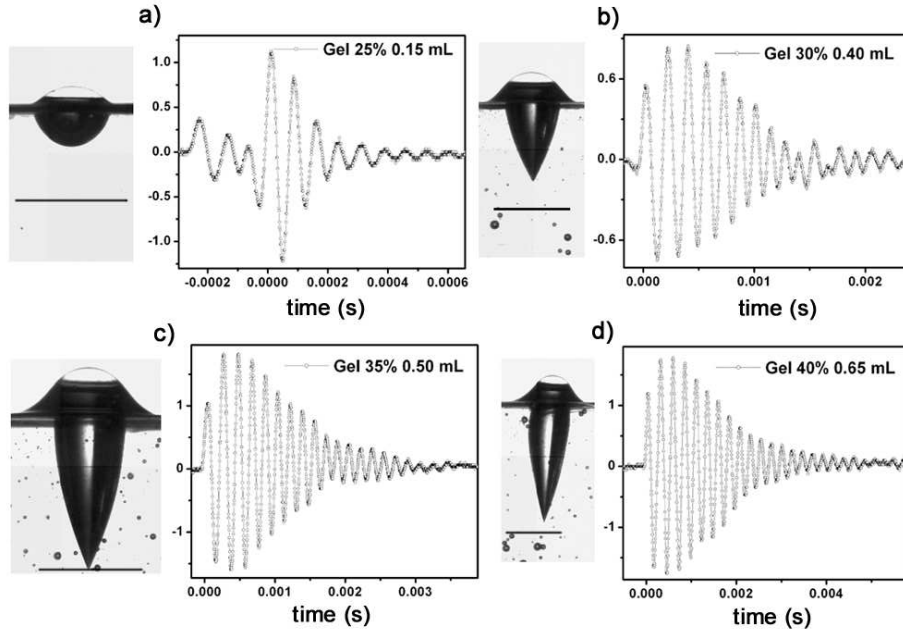


FIG. 5 – Typical bubbles shapes and associated signals, for 25, 30, 35 and 40 % gel concentrations. We can notice the decreasing frequency, and the increasing signal duration with bubbles volume. Black straight lines are worth 1 cm.

⁴This argument remains valid for a newtonian fluid with $\gamma_{eff} = \gamma_{water}$.

⁵A more quantitative approach is non trivial and would not teach us more, unless prove the unicity of the sharp shape of the bubble tail.

⁶typically for shape alike picture a) of figure 3.

We observe that the frequency emitted by the bursting bubble is directly linked to its length. More precisely, the frequency of the sound emitted is well defined, and corresponds to the fundamental mode of the tube corresponding to the tail of the bubble. The better way to see it is to plot the wavelength associated to the frequency recorded versus the length of the bubble.

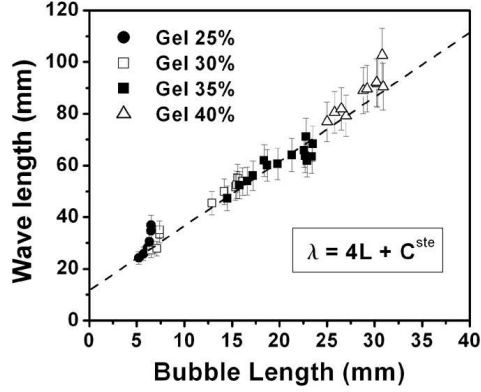


FIG. 6 – Wavelength (mm) of the sound emitted during the bubble bursting, versus the length L_b (mm) of the bubble. The linear fit is $\lambda = 4L + C^{ste} = 4(L + \delta L)$. δL can be interpreted as the real length of vibrating air, excited on the top of the bubble. Over this length, the plane wave existing in a tube is turned into a spheric wave radiated by the tube. For a radiating tube, δL is known to lie between $0.6R$ and $0.8R$ with R the tube radius, depending on the shape of the acoustic waveguide [23]. The ordinate at $L = 0$ gives $\delta L \simeq 2.5$ mm, thus $R \simeq 0.4$ cm which is the right rough estimate for our bubbles (see fig. 3).

For the open bubble, the closed end (tail) must be a displacement node, and the open end an antinode [3]. The distance between a node and the adjacent antinode is one-quarter of the wavelength of the travelling waves. We fairly observe a $\lambda = 4L$ law on figure 6. The point is that the elastic properties of the solutions allow the bubble to develop a centimetre tail which play the role of an *indeformable resonator excited by the breaking of the film*. Actually, the tearing of the thin film creates a sound wave which makes a round trip between the open horn and the bottom of the bubble, exciting a characteristic length of the bubble.

A way to see that there is really a characteristic length excited, evolving smoothly with the gel concentration of the solutions, is to compare the bubble to a tube $L_b \times S_b$ constructed with before-explosion bubble parameters.

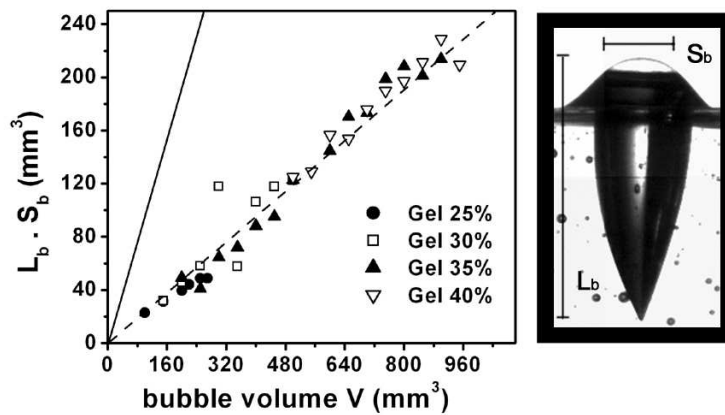


FIG. 7 – Left : comparison to the equivalent tube of the same length : length of the bubble before the thin film tears, times the largest section of the bubble at the same time, versus bubbles volume. The solid line is the first bissectrice representing an exact tube behaviour. Right : a 0.45 mL bubble in a 35 % Gel solution, on the edge of bursting, showing clearly before explosion's parameters L_b and S_b

Figure 7 shows us that changing the Gel concentration does not modify drastically the structure of the excited resonator. Furthermore, all solutions at different concentrations are part of the same straight line, which is not so trivial⁷ : for a given volume, but increasing the concentration, the bubble tail could present a pointed part more or less important than the cylindrical part. The curves associated would be more alike a log function or a power function respectively. There is some "universality" in the evolution of the effective resonating length as this evolution is the same for solutions of different Gel concentration. At this point, we can conclude that :

The bubble tail is a resonator, equivalent to a tube selecting frequency and excited by the film tearing. The part of the tail that is really excited seems to evolve independently of the Gel concentration and smoothly enough to be a relevant physical parameter.

This resonator property is firmly linked to elastic properties that set a sharp tail and introduce a time-scale large enough to allow the bubble tail being motionless during the sound emission. To be convinced, we can listen to the sound emitted by a bursting air-bubble at the surface of an aqueous solution of sugar (60 %) and compare the results with the ones obtained for the 30 % gel concentration solution of the same viscosity (fig. 8).

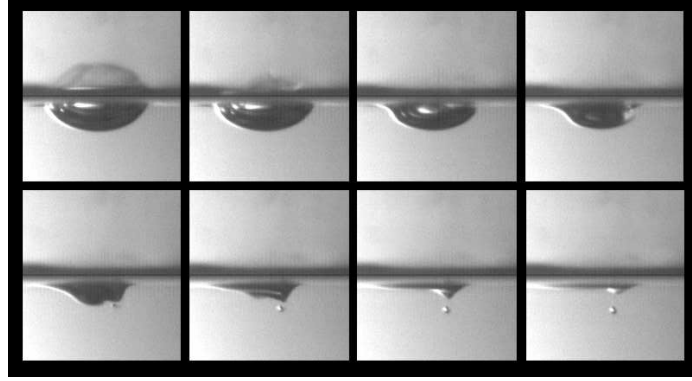


FIG. 8 – Air-bubble bursting at the surface of a 60 % sugar aqueous solution ($\Delta t = 1.6 \text{ ms}$).

Instead of being well defined, the frequency emitted by bubbles bursting on sugar aqueous solutions slides from 6.6 to 11.7 kHz, approximately. Energy is unequally distributed within both frequencies (fig. 9).

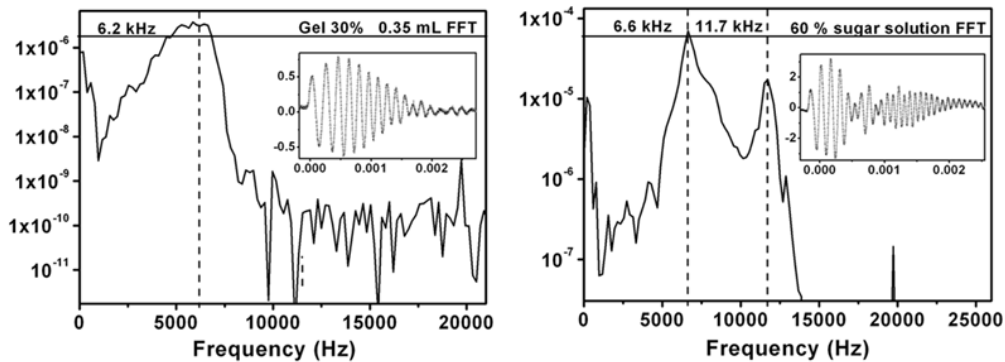


FIG. 9 – Right : FFT of the signal emitted by a 0.35 mL bursting bubble in a 30 % hair-Gel solution. Left : FFT of the sound emitted by a bursting bubble in a 60 % sugar solution. Original signals are given in both insets. Notice that the energy is concentrated and released monochromatically in the non-newtonian case.

⁷Actually, we are in the approximation of low frequency, as $\lambda = 4L \gg L$ or R , thus physics is less sensitive to the length ratio of the wave-guide.

In the non-newtonian case, the well defined resonator is excited by the film breaking (fig. 10) which will be discussed in detail in the next part. Roughly, the film breaking gives birth to an acoustic perturbation that propagates in two directions : a part of it propagates outside the bubble, while the other part is directed toward the bubble tail. The wave propagating inside the bubble may excite resonant mode of the cavity. A wave fairly exists in the bubble cavity as long as an overpressure ΔP remains in the bubble. We notice experimentally that the film breaking time remains shorter than the overpressure relaxation time.

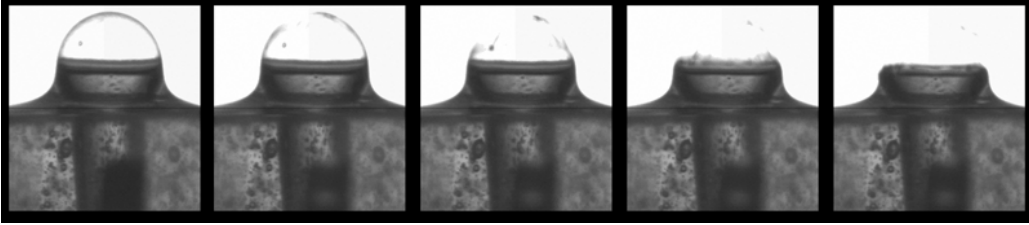


FIG. 10 – Pictures of the film breaking for a bubble in a 40 % Gel solution. This sequence corresponds to the duration of the sound emission ($\Delta t = 0.8 \text{ ms}$). Notice the surprising horn shape of bubble's top, not deformed during the sound emission. This figure is a good example of highly non trivial experimental result.

The case of a highly viscous film breaking with fast pressure equilibrium has been studied by Chaïeb Sahraoui at the MIT [29]. He used viscous polymer solutions ($\eta \simeq 10^3 \text{ Pa.s}$) to make a centimetre film break. As the viscosity is high, the breaking time τ_b is very long in front of the time needed to reach pressure equilibrium τ_P , and the film develops a large scale instability as it falls down under gravity as a falling big top (fig. 11).

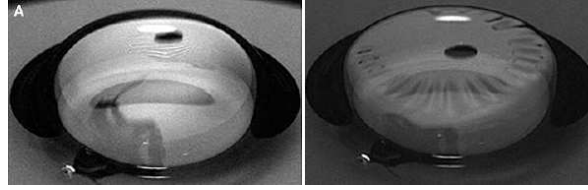


FIG. 11 – Film breaking of a very viscous polymer solution. Pressure equilibrium occurs before the complete film breaking leading to a large scale instability [29].

Let's finally notice that we also observe an instability already observed by Debregeas [9, 13], but completely different from Chaïeb's regime one. We observed a "parachute instability" due to the film buckling⁸ at the thickness scale.

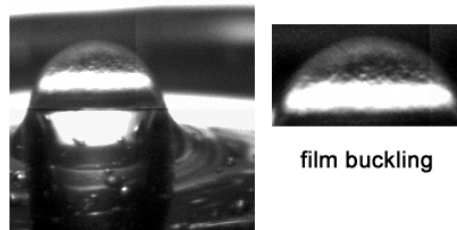


FIG. 12 – Small scale film instability ; right part is a zoom version of the enlighthed film. Gel 40%.

This comparison allows us to introduce the last characteristic time relevant for our bubbling issue : the equilibrium pressure time τ_P . Including the period T of the emitted signal, the film breaking time τ_b ,

⁸buckling could be translated in french by *flambage*.

and the total signal duration τ_S , we have all the relevant times of the problem that experimentally can be ordered as follows⁹ :

$$T \ll \tau_b \leq \tau_S \simeq \tau_P$$

We thus keep in mind that :

a bursting bubble can be mainly described with two characteristic time-scales : the sound period and the film breaking time.

And this as long as τ_P remains longer than any other time.

Through τ_b , the thin film tearing remains the excitation of our resonator. However τ_b is swamped by two other times. In order to test the influence of the excitation rate and to really understand it, we will work with a system very similar to bubbles, in which time-scales are more separated. Let's focus on the thin film tearing.

⁹ τ_b varies between 0.2 and 3 ms, while T varies between 0.07 and 0.2 ms.

II) Thin film story

The idea of this part is to focus on the excitation (the film tearing) of the resonator (the bubble tail). As we want to dissociate the film tearing from the natural characteristic times of the system, we used soap. The soap film breaking duration τ_b^{10} is the shortest time of the system as :

$$\tau_b \sim 0.1 \text{ ms} \leq T \sim 0.5 \text{ ms} \ll \tau_P \simeq \tau_S \sim 10 \text{ ms}.$$

The resonator is a tube made of plexiglas which constitutes a well defined and indeformable resonator. This system allows us to control uncontrollable bubble parameters as the film radius of curvature (overpressure) or the "bubble" geometrical properties. This way we will enlight the essential role played by τ_b .

II.1. Experimental setup

To focus on the film tearing, we handcrafted a simple plexiglas cell to listen to a film breaking under a well known overpressure. We use a "U-tube" of plexyglas which is halfly filled with distilled water. Under one tube we make a soap film using a razor strip thus trapping in an air volume demarcated by the distilled water and the soap film. We then inject air in this closed volume using a syringe. This way we control the inside-pressure, and the water-level change (Δh) in this very tube gives us the overpressure. We use the fast camera to get the level change with the required precision (typically, Δh is worth a few tenth of millimeter and varies during τ_b). Finally, by changing the level of distilled water in the U-tube before formation of the soap film, we control the resonating frequency of the tube under the soap film.

We made two cells as described, with different diameters : 4 and 8 milimeters. We show in figure 13 the grading of those tubes. The frequency emitted by the tube is plotted versus the opposite of the tube length recognizing the classic $1/L$ tube law [3,12]. At last, in inset we plot the wavelength emitted versus the tube length. The tube is opened at one end (pressure node) and closed at the other (velocity node). The distance between a node and the adjacent antinode is a quarter wavelength, which is easily verified ¹¹.

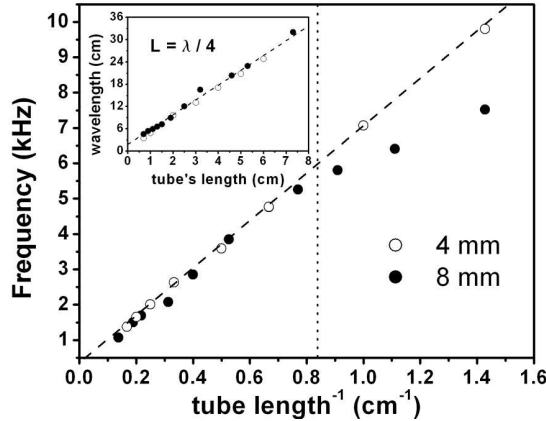


FIG. 13 – Frequency of the signal emitted by the tube versus the inverse of the tube length. Two tubes of respectively 4 and 8 mm of diameters are used. The classical $1/L$ law is verified in both cases. The deflection observed for the 8 mm diameter tube is linked to the effective length δL defined for figure 6 which is no longer small compared to L . The frequency emitted has to be written $\nu = c/4(L + \delta L)$. The 8 mm diameter tube which will always be used for length larger than 12 mm. Inset : wavelength emitted versus the tube length.

For the grading, the excitation of the tube are provided by the breaking of soap films, which are all lead to break the same original way : the chamber under the soap film is linked to a syringe of large

¹⁰ τ_b can be considered as a constant. Using a microscope we check that the film always breaks the same way.

¹¹The linear fit has got a not so surprising $0.15 = \frac{2 \times 0.3}{4}$ mm offset, which corresponds exactly to the fall of water level in the tube (0.3 mm) and the radius of the film on top of the cell (0.3 mm).

volume in front of the tube one. Just handing the syringe provides a thermal distention sufficient to push up the film and break it in a reproducible way.¹²

II.2. "Broken chord can sing a little"

Watching and listening to a film exploding over a tube, we control two parameters : the tube natural frequency, as we can change the level of water in the tube, and the excitation of the resonating tube, as we control the inner overpressure. A soap film tears in less than a few tenth of milisecond : $\tau_b \simeq 0.2 \text{ ms}$ meaning $\nu_b \simeq 5 \text{ kHz}$. We used tube of length ranging from 1 to 8 *cm*, meaning that the natural frequencies of our tubes range from 1 to 5 *kHz*. Thus, except for the smallest tubes, the system is always over-excited ($\nu_b \geq \nu_{tube}$).

We can than conduct two kinds of experiments. The first one consists in varying the excitation over a tube of given length, that is to say changing overpressure in the tube for a given level of water in the tube. The other one changes tube length for a given excitation. We begin with the last kind.

First, we choose a well defined excitation, and we change the resonator. We use tubes of different lengths excited by an exploding thin film, always submitted to the same overpressure Δh . The films are always made the same way using a razor strip, and using a large quantity of aqueous soap solution¹³. To sum up general results, let's take $\Delta h = 0.4 \text{ mm}$ for the tube of 8 *mm* diameter.

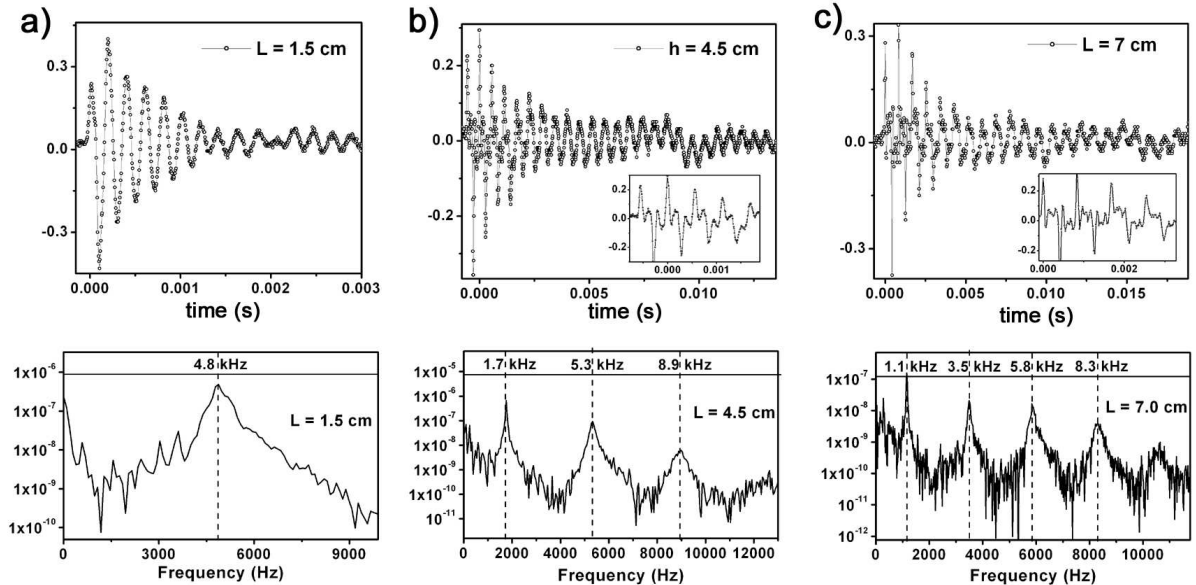


FIG. 14 – Up : typical signals emitted by different tubes of length : 1.5 & 4.5 & 7 *cm* excited the same way (overpressure fixed by $\Delta h = 0.4 \text{ mm}$). Down : corresponding FFT. We have for the three fft that the first two pics are in the ratio of 3 while the first and the third one are in the ratio of 5, etc. Insets : zoom on the non linearity for signal b) and c); time-scale : second.

Figure 14 gives 3 typical signals for tube lengths ranging from 1.5 to 7 *cm*, and the corresponding fft (for this excitation). For tube longer than 1.5 *cm*, we notice the presence of harmonics during the first oscillations of the signals. A zoom on these harmonics is given in inset for $L = 4.5$ & 7 *cm*. The Fourier transforms confirm us the presence of a large spectral contents for large tube. And that the energy is equally distributed in all the excited modes (only a decade of intensity between the first two modes, followings are equivalent). At this point, we cannot say more on the nature of the wave the tube contains.

¹²To break a film, the requested volume-increase is at max a half-sphere volume, i.e. $\delta V \approx 10^{-2} \text{ cm}^3$ for a our bubbles radius of a few mm. The corresponding temperature increase is then $\delta T \simeq T \frac{\delta V}{V} \simeq 0.3^\circ \text{C}$ for a 10 mL syringe volume. Increase easily provided by the human hand. Large volume V contains all the physics of this phenomenon.

¹³We verified using a microscope, that soap films always break the same way : draining make the film thinning until it reaches the newton black film.

Energy study will close the matter there.

We can also see on figure 14, that the tube is naturally a damped oscillator. After the film is broken, two main processes could be responsible for the dissipation. A sound is emitted (radiation), and the relaxation of the overpressure to zero is associated to an hydrodynamic flow from the in-tube to the outside generating a viscous dissipation. We have to define an energy we can access experimentally, this way we will see how the total energy is really stocked and dissipated.

II.3. Energy matter

Before dealing with energy, let's define the energy the microphone is sensitive to. A bursting bubble produces an acoustic wave. On the one hand, the power associated to the signal we record corresponds to the kinetic energy per unit time the microphone membrane is able to acquire : $\varepsilon_K \propto \rho v^2$, where ρ is the inertia of the membrane. On the other hand, the acoustic signal recorded $s(t)$ is proportional to the pressure fluctuations caused by the acoustic wave¹⁴ : $s(t) \propto p$. Finally, as for a propagative wave the pressure p is proportional to the wave speed v , we can fairly define¹⁵ the energy we listen to, *during the signal duration*, as :

$$E = \int_{\tau_S} (s(t) - \langle s(t) \rangle)^2 dt \quad (2)$$

We have to subtract the average level to be sure all signals, especially those of different experiments, can be compared. Practically, we have to be careful with the signal duration τ_S on which we make the integration. The oscilloscope always acquires 2000 points for each signal. the integration is discrete and includes the constant time delay Δt between 2 points, i.e. the acquisition frequency ν_a of the oscilloscope :

$$E = \sum_{2000 \text{ points}} (s(t) - \langle s(t) \rangle)^2 \cdot \Delta t = \frac{1}{\nu_a} \sum_{2000 \text{ points}} (s(t) - \langle s(t) \rangle)^2 \quad (3)$$

We defined an energy associated to the recorded signal in order to explain an "ear-catching" phenomenon : a highly curved bursting film is definitely noisier than a flat one. This fact leads us this time, for a given tube length to listen to the energy emitted by the soap film tearing with different radius of curvature. We used the tube of 8 mm diameter, which length is set at 5.5 cm. The syringe injecting the air into the tube is reset to the starting position for each film breaking. For each Δh , we took five measurements, in order to get three measurements with exactly the same Δh . On figure 15, each point is the average of three measurements.

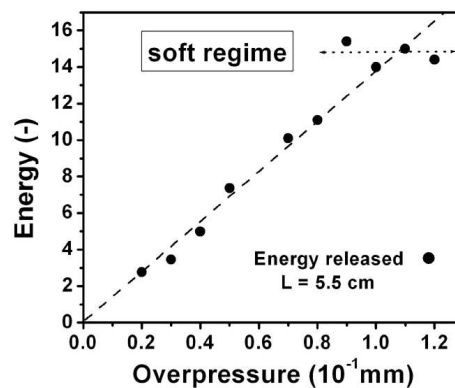


FIG. 15 – Energy emitted by a film bursting on a tube of given length (5.5 cm), versus the overpressure imposed. The energy is given with arbitrary units, in conformity with our definition.

¹⁴ Assuming the microphone is evolving in a linear regime.

¹⁵ Notice that except a factor $1/2\rho c$, this is the usual definition of the acoustic power per unit surface : $p^2/2\rho c$.

We notice two facts on graph 15 : the linearity of the energy recorded with the overpressure, and an increasing dispersion on the energy for the largest Δh :

The **linearity of the energy with the overpressure** may appear surprising. Our experiment can be understood as follows : a tube contains an overpressure ΔP , and is closed at both ends. At time $t = 0$, we open the right end (film tearing). Dealing with the problem linearly, the pressure step gives birth to two symmetric waves : one toward the bubble tail, and the other one toward the exterior. Writing f_+ and f_- the usual solutions of the d'Alembert equation, we find that the initial overpressure is symmetrically divided into two equal parts leading to the following wave velocity expression [17] :

$$v_{\pm} = \frac{\Delta P}{2\rho c} f_{\pm}(x \mp ct) \quad (4),$$

and the proportionality between the particles speed v and the overpressure ΔP inside the tube. And as the energy evolves with v^2 , we expect a linear dependance of the energy with ΔP^2 , and not ΔP . The only way to get a proportional relationship between v^2 and ΔP is to involve a non-linear mechanism. The shortness of the film breaking characteristic time in front of all other relevant timescales for the system, leads us to conclude that a shock wave occurs in the tube when the film breaks.¹⁶ Then writing the energy conservation on both sides of the shock wave front gives naturally¹⁷ :

$$\rho \langle v^2 \rangle \simeq \Delta P \quad (5),$$

leading the energy stocked in the cavity, being proportional to the overpressure :

$$E_{cav} \propto V. \Delta P \quad (6).$$

And as the losses in the tube are proportional to the energy stocked into the tube, we can easily understand that the energy we listen to is proportional to the overpressure (this fact will be well detailed in the next part II.4.). Producing the linear fit of energy to 0 (fig. 15), we can conclude that :

A flat film does not emit any sound : overpressure injects energy in the system {film-bubble} .

We can also notice an **increasing dispersion for the largest Δh** , which is not a new linear regime of different slope, but a *softer regime* before the film breaks. For our thin film generated over a closed tube, increasing the pressure decreases the radius of curvature, and makes the thin film well rounded. The radius of curvature of the thin film can decrease until reaching the tube radius (forming a hemisphere), as increasing it more make surface tension and overpressure evolve the same way. When the thin film is not far from half sphere shape, it responds softly to a pressure increase. A way to see this consists in evaluating, in the limit of high overpressure (Δh), the evolution of overpressure itself with a small volume increase.

The volume generated by a rounded thin film is : $V = \frac{2}{3} \pi R^3 (1 - \cos(\alpha))$, where R is the radius of curvature, and α the angle between the vertical and the film at the boundary (fig. 16). The radius of curvature is linked to overpressure by Laplace's law $\Delta P = 2\frac{\gamma}{R}$, and geometrically to the tube radius r_0 by $R \sin(\alpha) = r_0$. This allows us to write the volume V as a single function of ΔP :

$$V = \frac{2}{3} \pi \left(\frac{2\gamma}{\Delta P} \right)^3 \left[1 - \sqrt{1 - \left(\frac{r_0}{2\gamma} \right)^2 \Delta P^2} \right] \quad (7)$$

¹⁶this hypothesis is also fairly coherent with signals fft showing large spectral contents (fig. 14). We also notice the absence of non-linearity for a 1.5 cm tube (fig. 14.a) : the shock-wave front has a spatial extent of a few "acoustic particles" length. When this spatial extent is worth the tube length at a rough estimate, the tube becomes resonant, and the shock wave the fundamental $\lambda/4$ resonating mode.

¹⁷we forget on purpose numeric coefficients, as we henceforth focus on scaling laws.

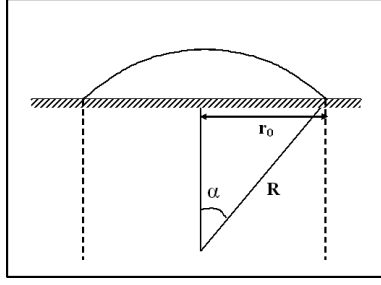


FIG. 16 – Graph giving the definitions of the relevant parameters needed to explain the soft regime of the film bent.

In the limit of high ΔP , $\frac{r_0}{2\gamma}\Delta P$ tends toward 1 as the curvature radius tends toward the tube radius. Setting $\frac{r_0}{2\gamma}\Delta P \equiv 1 - \epsilon$, with $\epsilon \ll 1$; we enlight physics rewriting the volume as following :

$$V = \frac{2}{3} \pi r_0^3 \frac{1}{(1 - \epsilon)^3} \left(1 - \sqrt{1 - (1 - \epsilon)^2} \right) \quad (8)$$

In the limit $\epsilon \rightarrow 1$, we have :

$$V \propto 1 - \sqrt{2\epsilon} + o(\sqrt{\epsilon}) \quad (9)$$

We thus evaluate the sensitivity to volume increase of a film of small curvature radius. We find that :

$$\left| \frac{\partial \epsilon}{\partial V} \right| \sim \sqrt{\epsilon} \ll 1 \quad (10),$$

meaning that for high overpressure regime, increasing the volume under the thin film do not affect its curvature. Thin film system is in a "soft regime". As soon as all the potential film curvature is used, the system is definitely less sensitive to an overpressure increase, and stocks less energy : this is another confirmation of the fact the overpressure contains the energy of the system.

Looking after the energy released on top of a tube of given length for different excitations leads us to understand the nature of the wave evolving in the tube : it is a shock wave exciting in a non trivial way several modes (fig. 14), and leading to a quadratic relationship between the particles velocity and the overpressure (5). We are also convinced now, that the bubble overpressure allows energy to be stocked (fig. 15).

However we do not know the way energy is dissipated, as two ways of dissipating energy exist : radiation and viscous dissipations. The next part will also help us to bring more proofs of the shock wave existence.

II.4. Energy balances

We want to write energy balances to evaluate which way energy is released from the system, whether by radiation or viscous dissipation. The signal duration, meaning the characteristic time for the sound signal to vanish, is a relevant parameter which is going to help us to write some scaling laws, and put us on the picture about energy evolution.

Writing down the total energy conservation law for an incompressible fluid, the viscous dissipation term occurs to be [14] :

$$\mathcal{P}_d = \iiint \sigma'_{ij} \frac{\partial v_i}{\partial x_j} dV \quad (11),$$

with σ'_{ij} the viscous stress tensor. This viscous dissipation takes place on a typical length $\delta \equiv \sqrt{\nu/\omega}$, with ν the kinematic viscosity, and ω a typical frequency. For a given tube, we choose ω as the lowest frequency the tube can emit. The power dissipated (11) can be rewritten dimensionally as follows :

$$\mathcal{P}_d \sim \eta \frac{v}{\delta} \cdot \frac{v}{\delta} \cdot \delta LR \quad (12)$$

δLR is the volume of a sleeve of the same length L and radius R that the tube, and thickness δ . Let's now make the assumption that the viscous dissipation is the main process of energy loss in our tube-film system and see what happens. The energy balance at the tube scale is :

$$\frac{d}{dt}(\rho V v^2) = -\frac{\eta}{\rho} \frac{v^2}{\delta} LR \quad (13)$$

Using the expression of the tube volume $V \simeq LR^2$, and substituting δ by its value, we find that :

$$\frac{dv^2}{dt} = -\left(\frac{\sqrt{\nu\omega}}{R}\right) v^2 = \frac{v^2}{\tau_{S\ vis}} \quad (14),$$

where $\tau_{S\ vis}$ is the viscous estimation of the signal duration. Notice that the signal duration varies as

$$\tau_{S\ vis} \propto \omega^{-1/2} \quad (15)$$

To confirm or infirm our assumption of a viscous driven process, we look at the signal duration evolution with the frequency. The experiment is lead as follow : the same overpressure is always imposed to films lead to burst on top of tube of different lengths. As some signals can be fit by a decreasing exponential, but some other cannot, we choose to collect the real signal duration, and not the characteristic decreasing time. We performed this experiment for 3 different overpressures. The real signal duration is plotted on graph 17 as a function of the frequency.

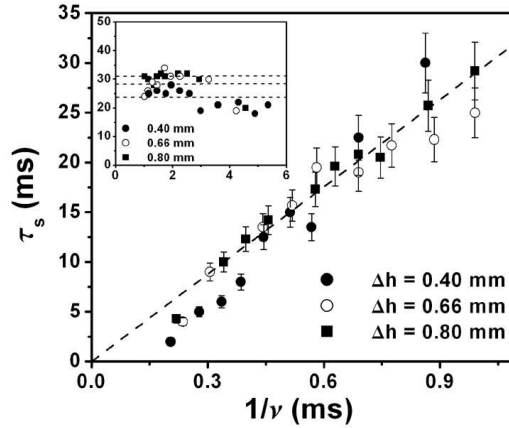


FIG. 17 – Signal total duration τ_s versus the inverse of the frequency recorded, for three different overpressures. Inset : number of oscillations versus the frequency (kHz).

The signal duration goes definitely linearly with the tube length L , and not as \sqrt{L} as would be the case if our assumption were right (remember, for a tube, $L \propto \omega^{-1}$). Another way to see the $1/\nu$ law is to plot the factor of quality of the tube defined as $Q = \omega \tau_s$ versus the frequency. Q is approximately the number of oscillations counted on a signal, and is here constant for a given excitation (Inset fig. 17).

We have to restate our assumption : energy losses are not driven by the viscous dissipation.

Let's thus have a look at the energy radiated at the top of the tube as soon as the film has broken. Evaluating the energy emitted at the end of the tube is really non trivial. A way introduced by L. Landau, regards the emitting end of the tube as a half vibrating sphere [19]. The energy per unit time emitted by a vibrating sphere depends on its volume acceleration \ddot{V} , and can dimensionally be reduced to :

$$E_{rad}|_t = \frac{\rho}{c} \langle \ddot{V}^2 \rangle \quad (16)$$

And if we write v_0 the mean particle speed at the opened end of the tube, we can consider the opened end as a gas source, with a flow $Sv_0 = \dot{V}$, with S the tube section. The energy emitted by unit time by the tube is then :

$$E_{rad}|_t = \frac{\rho S^2}{c} \langle v_0^2 \rangle \quad (17)$$

Now, the crux of the matter remains to write properly v_0 . As v_0 is yet a mean speed, v_0 has to be decomposed in a v_0 divided by a characteristic time. The energy is maximum when the acceleration does too; then the time on which we can expect pulsations at the end of the tube is the shortest time of the system : let's write it τ . Substituting v_0 by v_0/τ in the energy expression, we get the energy emitted by unit time at the end of the tube :

$$E_{rad}|_t = \frac{\rho S^2}{c} \frac{\langle v_0^2 \rangle}{\tau^2} \quad (18)$$

Using energy conservation (5), energy can finally be expressed as a function of the energy E_{cav} contained in the cavity before film breaking (6) :

$$E_{rad}|_t = \frac{S}{L} \frac{1}{c\tau} \frac{E_{cav}}{\tau} \quad (19)$$

Finally, assuming radiation to be the main process for energy loss in the tube, energy balance takes the following form :

$$\frac{d}{dt} E_{cav} = -E_{rad}|_t = -\frac{1}{\tau_{Srad}} E_{cav} \quad (20)$$

The tube section, and film breaking time are two constant parameters, we conclude that under the assumption of an energy loss driven by radiation, the signal duration varies like :

$$\tau_{Srad} \propto L \propto \omega^{-1} \quad (21),$$

which is exactly the scaling law experimentally encountered. Moreover the expression of τ_{Srad} is independent of ΔP which is in full agreement with the experiments (fig. 17).

In order to test our scaling law, we can deduce from the latest lines the radiated-energy variations with the tube frequency. This gives us a chance to see the self-coherence of our assumption. The total energy emitted is the radiated energy (19) integrated over the real signal length, that is to say :

$$E_{rad}|_{tot} = \frac{S}{L} \frac{1}{c\tau^2} E_{cav} \times \tau_{Srad} = SL \Delta P \quad (22)$$

On figure 18, we verify that the radiated energy varies as the length of the tube. The experiment is conducted for 2 different overpressures and the ratio of the two linear fits equals approximately the overpressure ratio. The radiated energy is fairly proportional to the volume and the overpressure.

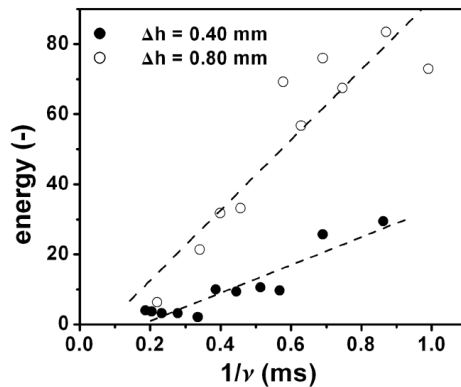


FIG. 18 – Energy emitted by tubes of different lengths submitted to the same excitation ($\Delta h = 0.40$ & 0.80 mm). The slopes of the linear fit are in ratio of 2, equal to the overpressure ratio.

Finally, we have introduced τ , the shortest time-scale of the system. We chose to note it τ as it does not play any role in our scaling laws, except by being constant¹⁸. However, τ_b the film breaking-time is a suitable candidate for that time τ .

II.5. Soap conclusions

The energy is stocked in the tube because of the overpressure we inject, which one leads to curve the film. In that sense, curvature contains the energy. Energy emitted goes also linearly with the overpressure and the tube length that allows us to propose a last expression for the energy associated to the emitted signals :

$$E = f\left(\frac{\tau_b}{T}\right) V. \Delta P \quad (23)$$

In expression (23) we introduce f as a slowly variable function of τ_b . Indeed, the film breaking time τ_b is not a perfect constant, and certainly evolves slowly with overpressure and tube length. However, τ_b remains the shortest time of the system, and drives the energy dissipation process : mainly radiation.

¹⁸or slowly variable, as long as the variations of τ are small compared to the next shortest characteristic time in the system.

III) Back to bubbles

In this part, we get back to the bubble study, keeping in mind soap films results. The purpose is here to focus on the way the bubble tail (resonator) is excited by the film breaking, which time-scale is no longer the shortest and limiting time-scale of the system. Even slowly variable, the time of the film breaking τ_b enters in competition with the other time-scales allowing a brandnew behaviour for the energy associated to the emitted signals. As overpressure is not a well controlled parameter of the system {bubble}, we begin directly with energy matter.

III.1. Linear burstings

We saw that for a soap film bursting, the energy is released quasi-equally between the excited modes and that only a decade gap can be observed between the first two modes. A shock wave taking place during the film breaking is the only explanation for the energy to be released such a way. This is not the case for bubbles. Fast Fourier Transform shows us on figure 9 and especially 19, that the harmonics modes only begin to be significantly excited from 40 % Gel solution, and that at least a 2 decades gap of intensity separates the first two modes.

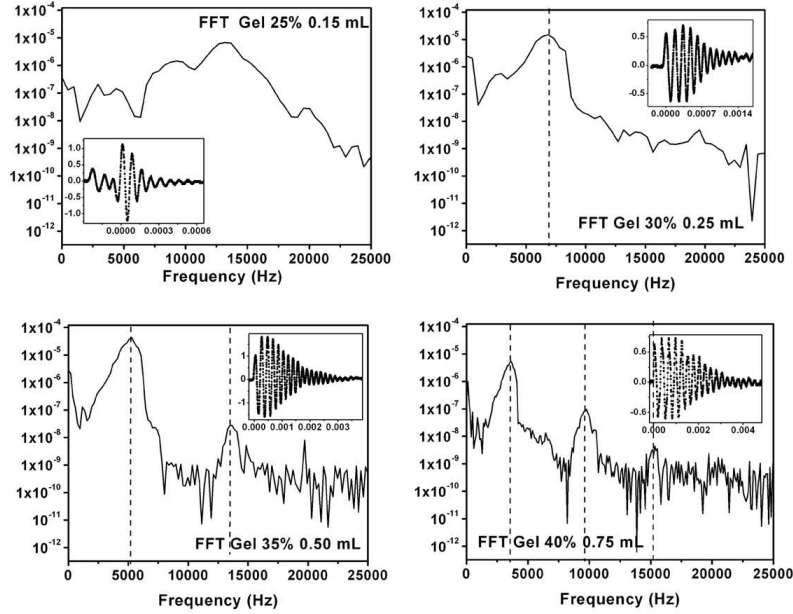


FIG. 19 – Characteristic FFT of signals emitted by bubbles of increasing volume at the free surface of Hair-Gel solution of increasing concentration. Scale is the same for the whole four graphs. Insets : corresponding signals ; time-scale is the second.

On the one hand, the signals emitted in the 25 % Gel solution present a large spectrum certainly linked to the water-like properties of the solution, which allow spherical shapes for the bubble. On the other hand, bubbles bursting at the free surface of a solution of 40 % Gel concentration seems to present a similar behaviour to a tube, but excited at lower frequencies as the film breaking times are longer ($\tau_b \geq 1.6 \text{ m.s}$) than soap ones ($\tau_b \leq 0.2 \text{ m.s}$). Between this two cases, Gel 30 and 35 % solutions exhibit strong monochromatic behaviours. Whatever, in the whole range of frequency we use, the harmonic are excited such a weak point, we can consider the problem as linear, meaning that the particles speed is proportional to the overpressure inside the bubble.

From now on we do not expect the same quantitative behaviour between the soap-film device and exploding bubbles.

III.2. "Sweet and Lowdown"

In Part II, we showed that a plexiglas tube excited by the breaking of a soap-film is a damped oscillator *over-excited*. Consequently, plotting the energy versus the frequency emitted by the resonating tube, we obtain a decreasing shape (fig. 18) : the soap-film breaks very quickly in front of the period of the signal a the tube can produce. In the case of the exploding bubbles, the breaking-time of the film evolves with the Gel concentration ($\simeq 0.2$ to 4 ms), but always remains larger than the period of the signal a bubble can produce. We would thus expect an increasing shape.

The figure 20 shows the energy released by bubbles bursting versus the frequency emitted. Curves associated to longer bubbles (35 and 40 % Gel concentration) present a surprising "hat shape", i.e. a **resonance**. If "hat-shape" curves present only a few points on the decreasing side, the decreasing side experimentally really exists, and remains unclear. Nevertheless, we can present here some results giving an intuition about what's going on.

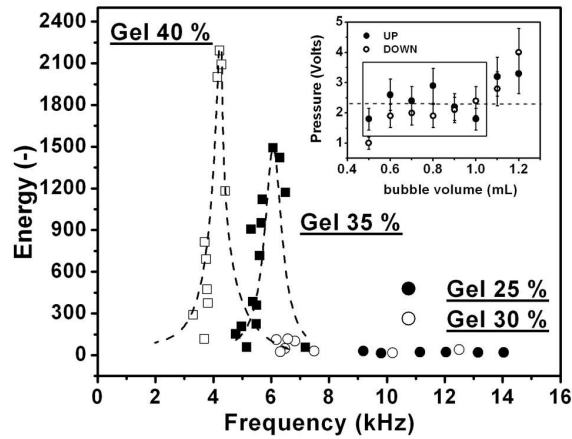


FIG. 20 – Energy recorded while bubble bursting, versus the frequency emitted. Dashed lines are only here as an eye-guide. Experiments are performed for 4 Gel concentrations : 25, 30, 35 and 40 %. Inset : the bubbles overpressure for a 40 % Gel solution. To ensure the reproducibility of the results, the curve is made two times, the first one increasing the bubbles volume (UP), the second one decreasing the bubbles volume (DOWN).

We can see what results the scaling law developed in the latest part gives us ; we still want to make an energy balance, and more precisely write a balance about E_{cav} , the energy stocked by the bubble tail. We still can write the volume variation as the flow getting out of the bubble $\dot{V} = S.v_0$. And as here the shortest time of the system remains the signal period, the energy radiated per unit time can be written :

$$E_{rad}|_t = \frac{\rho S^2}{c} \langle v_0^2 \rangle = \frac{\rho S^2}{c} \omega^2 \langle v_0^2 \rangle \quad (24)$$

Using that v_0 and ΔP are proportional (III.1.), energy can be expressed as a function of the energy E_{cav} contained in the cavity before film breaking (6) :

$$E_{rad}|_t = \frac{\rho c}{L^4} V^2 \Delta P^2 = \frac{\rho c}{L^4} E_{cav}^2 \quad (25)$$

Finally, assuming radiation to be the main process for energy loss in the tube (II.), energy balance takes the following form :

$$\frac{d}{dt} E_{cav} = -E_{rad}|_t = -\frac{\rho c}{L^4} E_{cav}^2 \quad (26)$$

Integrating (26) over the signal timescale τ_S , the energy in the cavity and thus released varies as follows :

$$E_{cav} \propto \frac{L^4}{\tau_S} \propto L^2 \quad (27)$$

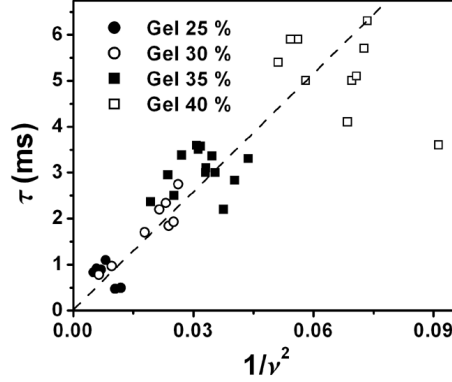


FIG. 21 – Signal total duration τ_S versus the square of the frequency recorded, for 4 different Gel concentrations.

We find experimentally the L dependance for τ_S (fig. 21). This scaling-law argument explains the increasing shape of the energy emitted with the frequency : the limiting time-scale of the system is no longer slowly variable compared to the other time-scales. However, we cannot explain the decreasing part of the graph this way. Another effect has to be taken into consideration.

We check **the reproductibility of the thin film breaking**, exactly as we did for the soap-films. Using a microscope, we convinced ourselves the film breaks a non trivial, but reproducible way, whatever the Gel concentration of the solution is. A typical breaking sequence is reproduced on the figure 22.

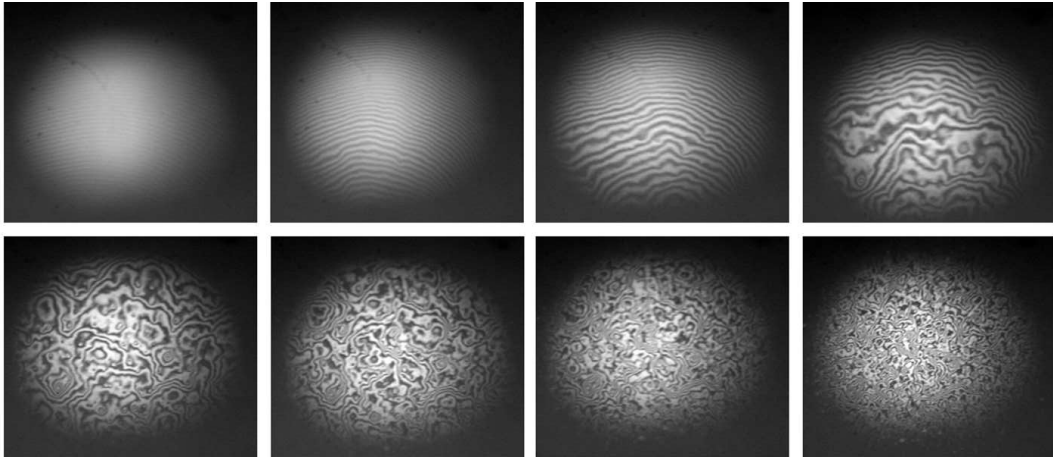


FIG. 22 – Pictures of the film breaking with a microscope ($\Delta t \approx 15$ s). The thin film first shows an interference figure, exactly as a soap-film does. Then the film becomes more and more wrinkeld showing complex figures, till the film breaks.

We check **the evolution of the overpressure inside the bubbles with a volume increase**. For a 40 % Gel solution, we measure the overpressure in the bubbles with a static pressure captor, fixed parallel to the tube supplying in air the submerged orifice creating bubbles in our Gel column. The bubble liberation triggers a depressure which intensity is recorded with a oscilloscope. We plot the maximum obtained varying the volume of the bubbles in the inset of figure 20. Contrary to energy, there is no abrupt evolution of the overpressure with the volume increase. The pressure remains constant in the range of volumes used to plot the 40 % energy curve. *The overpressure seems not to explain the hat-shape energy curves.*

III.3. High frequency conclusions

A bursting bubble is a resonating tube excited by the film breaking. Although the film breaking time-scale remains largest than the period of the signal emitted by the bubble, the evolution of the energy released with the bubble length is non trivial. We observe a resonance which cannot be explained by the complex breaking process of the thin film, or the strong overpressure necessary to create a bubble and make it rise.

We do think this "hat-shape" effect is due to a pure resonance effect inside the tube. Geometrical parameters adjust themselves such a way the energy released is maximal only for a set of parameters. The question remains opened.

After dwelling on the highest frequency over three parts, we can now legitimately focus on the lowest frequency.

IV) The low frequency

We focused lately on the low frequency which is not a mystery as being easily visible while performing experiments dealing with the high frequency. Indeed, this low frequency appears to be a **shear elastic wave**, produced by the bubble collapse, and shaking the highest part of the hair-Gel column. The Gel column used is the same as described in part I., and has been extended on top by a 8 cm diameter and 3 cm depth cylinder, in order not to be limited by the edge of the cell.

In a newtonian fluid a collapsing bubble produces a surface wave. The bubbles inner-wall fall down on each other, generating a draught excluder of increasing diameter going away from the collapsing point. On figure 23 we produce shots of a movie realised with a 60 % sugar aqueous solution where the expansion of the draught excluder is clearly visible.

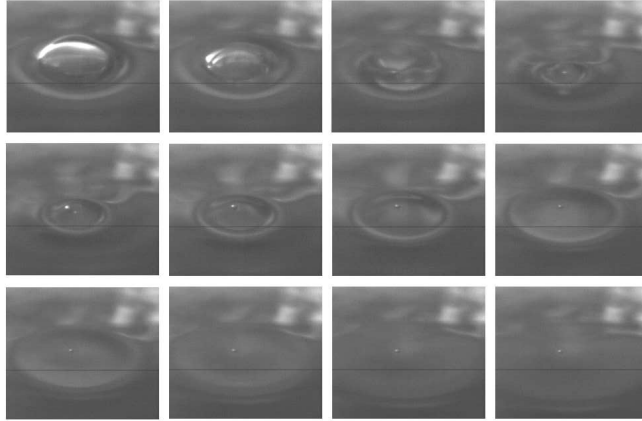


FIG. 23 – expansion of the draught excluder created by a bursting bubble at the free surface of a 60 % sugar aqueous solution.

In the non-newtonian case, the bubble collapses and recoils generating the same surface wave that in the newtonian case. The elastic properties of the solutions allow a response of the Gel to the bubble collapse, which consists in a *shear elastic wave* of a few centimeters depth from the free surface, and a very few centimeters extension. Oscillations of the small bubbles remaining in our solutions allow us to detect this shear wave, and that is also a rough estimate mean to get the elastic wave frequency. Small bubbles are injected underneath the free surface on purpose in a Gel solution. The radius should not exceed a few millimeter so that small bubbles will keep its shapes. Figure 24 shows the oscillations of two single bubbles while the wave pass through them. We find an approximate frequency of 15 Hz.

Notice that a simple surface wave is unable to produce such oscillations, but only excite the shear elastic wave. The frequency associated to a simple surface wave generated by the collapse of bubbles of a few centimeters length would be inferior to the frequencies we find experimentally, and would not depend on the Gel properties. Indeed, the frequency of a surface wave generated by a 2 cm length collapsing bubble is :

$$f = \frac{1}{2\pi} \sqrt{gk} = \frac{1}{2\pi} \sqrt{g \frac{2\pi}{L}} \simeq 9 \text{ Hz} \quad (28),$$

with g the gravity and L the bubble length.

Another argument consists in evaluating the product $f \tau_{dissipation}$ which compares the dissipation time-scale to the surface wave time-scale as follows :

$$f \tau_{dissipation} \sim \frac{f}{\nu k^2} \sim 5.10^{-3} \ll 1 \quad (29),$$

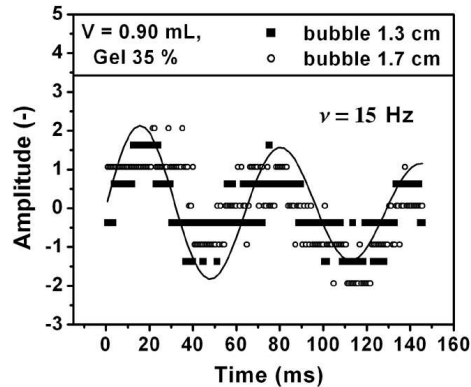


FIG. 24 – Single bubble oscillations due to the passing by elastic wave. The bubble is shot with the fast camera, its position noted down for each frame. Wave displacement is rebuild this way. The job is done for 2 bubbles; their respective distances to the collapsing point are indicated in centimeter. The fit is obtained minimizing the only frequency.

using a viscosity of approximately $10^5 \nu_{water}$. We thus conclude a simple surface wave is quickly dissipated and cannot be the motor of the Gel vibration.

However this method of following a single oscillating bubble does not give access to the wave amplitude decrease¹⁹, and remains rough to get the frequency accurately. A more appropriate method consists in enlightning a given point of the Gel-solution free surface with a laser beam. Beforehand the free surface have been smoothed out, and the laser beam widen out such a way we obtain a straight laser line reflecting on the free surface²⁰. The reflected laser line hit a displacement detector. When the elastic wave come by, the detector allows us to follow the surface oscillation in a given point.

We first fixed our extended laser beam on a given area, and make bubbles of different volumes explode at the free surface of a 35 % Gel solution. Between each bubble, the solution is stirred, as we still focus on non-presheared solutions. On figure 25, surface oscillations obtained with the laser method are plotted for three different volumes of exploding bubbles.

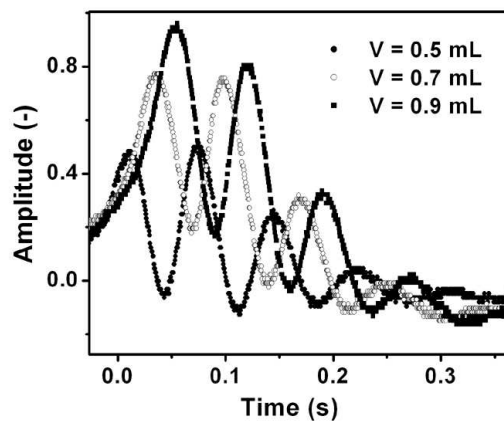


FIG. 25 – The surface oscillations on a given point due to the the shear elastic wave passing by. We change the volume of the exploding bubble, and so the intensity of the excitation.

¹⁹A good idea would be to inject bubbles of a few millimeters radius on an imaginary line drawn from the colapsing point to an edge of the cell. Determining the amplitude of each bubble would gives us the decrease of the wave amplitude. After several attempts, results are not enough accurate to achieve our purpose.

²⁰A cylinder of plexyglas is sufficient to transform a focused laser beam in a thin laser brush.

We observe that the resolution of the signal is quite good, and the decreasing amplitude is fairly visible. Increase the bursting bubbles volume naturally increase the amplitude of the first pic, and does not change the elastic wave frequency. For a 35 % Gel solution, we find 14.0 Hz , and a 40 % Gel solution gives approximately a 15.5 Hz . Generally speaking, the low frequency increases, and becomes to slide being less well-defined with increasing Gel concentrations. However, it remains between 10 and 20 Hz for concentrations going from 30 to 60 %.

Finally, a shear elastic wave satisfy the same equation of propagation as an acoustic wave ; a balance of forces for a slice of Gel of depth h , width dx and elastic modulus κ can be written as follows :

$$(\rho h dx) \frac{d^2 z}{dt^2} = \kappa \frac{d^2 z}{dx^2} (h dx) \quad (30)$$

The emerging frequency is thus :

$$f \sim \frac{c_{shear}}{L}, \text{ with } c_{shear} = \sqrt{\kappa/\rho} \quad (31).$$

This simple dependance of the frequency with L is compatible with the increase of the frequency with the Gel concentration. The usual shear modulus of our Gel solutions is approximately 100 Pa ²¹, which gives a fair frequency of $f \simeq 15 Hz$ for a 2 cm length bubble.

²¹This measure has been done in Lyon by J.-C. Geminard, using a rheometer.

Conclusion and Outlook

We are now convinced that :

a bursting bubble at the free surface of a non-newtonian fluid can produce two well defined frequencies.

The highest, and audible one (a few kHz) is produced by the excitation of the bubble tail which plays the role of a resonator. The frequency is driven by the bubble-tail length exactly as a tube does and the breaking of the thin film separating the bubble from the bulk air is the excitation. When the bubble collapses, a shear elastic wave is generated which involves the Gel solution properties. This low frequency is slowly dependant of gel properties and is worth about $15 Hz$. Finally, an esthetic result is that both frequencies can be written as a function of bubble length L : $f_{high} = c_{air}/4L$, while $f_{low} = c_{Gel}/L$. In order to enlight characteristic-times competition, we developed a simple device to listen to soap-film bursting on top of plexiglas tubes. By this way we confirmed that the shortest time (τ_b for a soap film, T for the bubbles) of the system play an essential role in the oscillator response. This device is also a very simple way to define, and deal with energy matter : energy is released by radiation in the case of a motionless resonator. However, optimal conditions for the energy to be released from a bursting bubble remains to be clearly explained.

Being curious, we conducted some experiments in permanent regime we did not mentioned explicitly in this report ; bubbles are emitted at a given frequency at the bottom of the cell and the hair-Gel solution *not stirred* between two emissions. Bubbles rise and explode without making a stop on top of the Gel column, whatever the concentration is. As the bubbles are longer (fig. 2, comment), the frequency is lower, usually $1 kHz$ above our results, but the same well defined one for all bubbles. In this regime, bursting bubbles always leave in addition a small bubble underneath the free surface exploding-point, meaning the bursting bubble does not empty itself completely. The following bubbles usually collapse with the left bubble. And if they collapse while the thin film of the upper bubble is tearing, not only one, but two high frequencies are emitted (chronologically the first one is always lower than the second one). This simple result remains another source of explanations for volcanologists.

A study varying the frequency of bubble emission, recording and correlating the frequency emitted remains to be done ; also that a complete study on sound emitted by underneath-the-surface collapsing bubbles.

TABLE OF FIGURES

FIG.1 : The Weissenberg effect (Left) and "die swell effect" (Right), [Bird].

FIG.2 : A rising bubble in a 40 % hair-Gel solution ; left : in a non-presheared solution ; right : in a presheared solution.

FIG.3 : Bubble shapes for 3 concentrations and 4 representative volumes.

FIG.4 : The bubble length before explosion L_b versus the bubble volume V , for 25, 30, 35 and 40 % Gel concentration.

FIG.5 : Typical bubble shapes and associated signals for 25, 30, 35 and 40 % Gel concentration.

FIG.6 : Wavelength of the sound emitted during the bubble bursting, versus the bubble length before explosion L_b .

FIG.7 : The bubble parameters before explosion versus the bubble volume : smooth evolution of the effective resonating length.

FIG.8 : Air-bubble bursting at the free surface of a 60 % sugar aqueous solution.

FIG.9 : Comparison between the signal emitted by a 0.35 mL bursting bubble at the free surface of a hair-Gel solution and the same process at the free surface of a viscous-equivalent sugar aqueous solution.

FIG.10 : Pictures of the film breaking for a bursting bubble at the free surface of a 40 % Gel solution.

FIG.11 : Film breaking of a very viscous polymer solution. [Chaieb]

FIG.12 : Film Buckling. 40 % Gel solution.

FIG.13 : Frequency of the signal emitted by the tube versus the inverse of the tube length. Inset : wavelength versus the tube length.

FIG.14 : Typical signals emitted by different tubes of length 1.5, 4.5 and 7 *cm*, and the corresponding FFT.

FIG.15 : Energy emitted by the film bursting on a tube of given length (5.5 *cm*), versus the overpressure.

FIG.16 : Graph giving the definitions of the relevant parameters needed to explain the soft regime of the film bent.

FIG.17 : Signal total duration τ_S versus the inverse of the frequency recorded, for three different overpressures. Inset : number of oscillations versus the frequency.

FIG.18 : Energy emitted for tubes of different lengths, and submitted to the same excitation ($\Delta h = 0.40$ and 0.80 *mm*).

FIG.19 : Characteristic FFT signals emitted by bursting bubbles of increasing volume, at the free surface of different Gel solutions. Inset : corresponding signals.

FIG.20 : Energy recorded while bubbles burst, versus the frequency emitted. Inset : evolution of the overpressure inside the bubble with the volume for a 40 % Gel solution.

FIG.21 : Signal total duration τ_S versus the square of the frequency recorded, for 4 different Gel concentrations.

FIG.22 : Expansion of the draught excluder created by a bursting bubble at the free surface of a 60 % sugar aqueous solution.

FIG.23 : Pictures of the thin film breaking with a microscope ($\Delta t \approx 15 s$).

FIG.24 : Single bubble oscillations due to the coming by elastic wave (Direct method).

FIG.25 : Single bubble oscillations due to the coming by elastic wave (Indirect method).

BIBLIOGRAPHY

- [1] Y. Amarouchene, *Thèse : Etude de l'interaction polymère-écoulement*, Université Bordeaux I (2002)
- [2] Y. Amarouchene, D. Bonn, J. Meunier and H. Kellay, Inhibition of the finite time singularity during droplet fission of a polymeric fluid, *Phys. Rev. Lett.*, **86**, 3558 (2001)
- [3] J. Backus, *The Acoustical Foundations of music*, W. W. Norton & Company, New York (1969)
- [4] A. Belmonte, Self-oscillations of a cusped bubble rising through a micellar solution, *Rheol. Acta*, **39**, 554-559 (2000).
- [5] R.B. Bird, R.C. Armstrong and O. Hassager, *Dynamics of polymeric liquids (vol 1 and 2)*, Wiley, New York (1987)
- [6] S.J. Candau, E. Hirsch, R. Zana and al. Rheological Properties Of Semidilute And Concentrated Aqueous-Solutions Of Cetyltrimethylammonium Bromide In The Presence Of Potassium-Bromide, *Langmuir*, **5**, 1225-1229 (1989)
- [7] M. Cates, *Macromolecules*, **20**, 2289 (1987)
- [8] M. Cates, S.J. Candau, Statics And Dynamics Of Worm-Like Surfactant Micelles *J. Phys. Cond. Mat.*, **33**, 6869-6892 (1990)
- [9] G. Debregeas, P.-G. de Gennes and F. Brochard-Wyart, Life and death of a bear viscous bubble, *Science*, **279**, 1704-1707, (1998)
- [10] G. Debregeas, P. Martin and F. Brochard-Wyart, Viscous Bursting of Suspended Films, *Phys. Rev. Lett.*, **75**, 21 (1995)
- [11] J. Drappier, T. Divoux, and al, Turbulent drag reduction by surfactants, *To be published*
- [12] N.H. Fletcher and T.D. Rossing, *The Physics of musical instruments*, Springer Verlag (1998)
- [13] P.G. de Gennes, F. Brochard-Wyart, D. Quéré, *Gouttes, bulles, perles et ondes*, Belin, Paris (2002)
- [14] E. Guyon, J.P. Hulin and L. Petit, *Hydrodynamique physique*, nouvelle édition, EDP Sciences, CNRS Editions Paris (2001)
- [15] N. Z. Handzy and A. Belmonte, Oscillatory rise of bubbles in wormlike micellar fluids with different microstructures *Phys. Rev. Lett.*, **92**, 124501 (2004).
- [16] A. Jayaraman and A. Belmonte, Oscillations of a solid sphere falling through a wormlike micellar fluid *Phys. Rev. E*, **67**, 65301-65304 (2003).
- [17] J. A. Kemp, *PhD thesis : Theoretical and experimental study of wave propagation in brass musical instruments*, University of Edinburg (2002)
- [18] I.L. Kliakhandler, Continuous chain of bubbles in concentrated polymeric solutions *Phys. Fluids*, **14**, 10, (2002)

- [19] L. Landau and E. Lifchitz, *Mécanique des fluides*, Edition Mir, Moscou (1989)
- [20] H. Z. Li, Y. Mouline, N. Midoux Modeling the bubble formation dynamics in non-Newtonian fluids *Chem. eng. Science*, **57**, 339-346 (2002).
- [21] H. Z. Li, X. Franck, D. Funfschilling, P. Diard, Bubble rising dynamics in polymeric solutions *Phys. Lett. A*, **325**, 43-50 (2003).
- [22] H. Z. Li, X. Franck, D. Funfschilling, Y. Mouline, Towards the understanding of bubble interactions and coalescence in non-Newtonian fluids : a cognitive approach *Chem. eng. Science*, **56**, 6419-6425 (2001).
- [23] A. Pierce, *Acoustics, An Introduction to its Physical Principles and Applications*, ASA, New-York (1989).
- [24] M. Ripepe, Evidence for gas influence on volcanic seismic signals recorded at Stromboli, *J. Volcanol. Geotherm. Res.*, **70**, 221-233 (1996)
- [25] M. Ripepe, S.Ciliberto and Della Schiava, Time constraints for modelling source dynamics of volcanic explosions at Stromboli, *J.Geophys. Res.*, **106**, 8713-8727 (2001)
- [26] M. Ripepe and E. Gordeev Gas bubble dynamics model for shallow volcanic tremor at Stromboli, *J. Geophys. Res.*, **104**, 10639-10654 (1999)
- [27] M. Ripepe, A J.L Harris, R. Carniel, Thermal, seismic and infrasonic evidences of variable degassing rates at Stromboli volcano *J. Volcanol. Geotherm. Res.*, **118**, 285-297 (2002)
- [28] T. Shikata , H. Hirata and T. Kotaka, Micelle Formation Of Detergent Molecules In Aqueous-Media 1, 2, 3 and 4, *Langmuir*, **3**, 1081 (1987); *Langmuir*, **4**, 354-359 (1988); *Langmuir*, **5**, 398-405 (1989); *J. Phys : Chem*, **94** , 3702-3706 (1990)
- [29] R. da Silva, S.Chaïeb and L. Mahadevan, Rippling Instability of a collapsing Bubble, *Science*, **287**, (2000)
- [30] S.Vergniolle and G.Brandeis, Strombolian explosions, 1. A large bubble breaking at the surface of a lava column as a source of sound, *J.Geophys. Res.*, **101**, 20433-20447 (1996)
- [31] S. Vergniolle, G. Brandeis and J.-C. Mareschal, Strombolian explosions, 2. Eruption dynamics determined from acoustic measurements *J.Geophys. Res.*, **101**, 20449-20466 (1996)
- [32] S. Vergniolle and G. Brandeis, Origin of the sound generated by strombolian explosions, *Geophys. Res. Let.*, **21**, 1959-1962 (1994)
- [33] V. Vidal, F. Melo, J.-C. Geminard and al., Sounds emitted by bursting bubbles (permanent regime), *To be published*